Design and Control of the Nonholonomic Manipulator

Yoshihiko Nakamura, *Member, IEEE*, Woojin Chung, and Ole Jacob Sørdalen, *Member, IEEE*

***Abstract*—Nonholonomic constraints are exploited to design a controllable n-joint manipulator with only two inputs. Gears subject to nonholonomic constraints are designed to transmit velocities from the inputs to the passive joints. The system possesses a triangular structure for which a conversion into chained form is presented. The nonholonomic manipulator can, therefore, be controlled with an open loop or a closed loop using existing controllers for chained form. Mechanical design is established, and experimental results proved the usefulness of design of the nonholonomic manipulator and applied control schemes.**

While previous publications have assumed that the nonholonomic systems are given and have developed theory for these systems, this paper points out a new direction where the nonholonomic theory is used to design controllable and stabilizable systems.

***Index Terms*—Chained form, nonholonomic constraint, nonlinear control, robot manipulator, underactuated system.**

I. Introduction

RECENTLY, the nonholonomic mechanical systems have received much attention in the field of robotics and control engineering. Many theoretical developments have been accumulated in particular for driftless systems and prepared as powerful tools. The scope of this paper is the definitions and developments of the new nonholonomic machines that function on the basis of nonlinear control theory.

The start point of this study is to explore the possibility of innovative and useful mechanisms from the nonlinear control theoretic background. While previous publications have assumed that the nonholonomic systems are given and have developed theory for these systems, this paper points out a new direction where the nonholonomic theory is used to design controllable and stabilizable systems.

Nonholonomic systems are typically controllable in a configuration space of higher dimension than that of the input space. The particular goal of this study is design and control of a manipulator consisting of n revolute joints using only two actuators, exploiting the unique feature of nonholonomic systems. The major flow of discussions goes in the order of theoretical design of the nonholonomic manipulators, development of nonlinear control strategies, and experimental verifications.

There are many interesting nonholonomic mechanical problems, such as kinematic integrating machines in [29] and [30], rolling contact between objects in [18] and [21], and manipulation by pushing in [20], [1]. Other typical examples are space robots in [27] and [44] and underwater vehicles [28]. Recently, there have been several works on designing new mechanisms using the nonholonomic constraints [31], [9], [51], [19]. The basic concept of the nonholonomic manipulator was proposed in [6], which was the start point of this paper.

Among the many works on the nonholonomic systems, works related to wheeled mobile robots and its applications are directly related to this paper. Controllability analysis were shown in [17] and [16]. Motion planners for low-dimensional systems were studied in [11] and [33]. On the other hand, control theoretic approaches were made based on differential geometric framework for general nonholonomic systems. Murray and Sastry [26] proposed a chained form, which is a canonical form for a class of driftless nonholonomic systems. Sørdalen showed conversion of a mobile robot with n trailer system to the chained form [37], [38]. Many open-loop controllers were proposed for the driftless systems including the chained form, such as [26], [47], [24], [15], and [46]. Other useful canonical forms were proposed such as the Goursat normal form [4], [25], [47] and the power form [22], [13].

There are fundamental difficulties on the feedback controller design of the nonholonomic systems, well known as the Brockett's theorem [3]. Therefore, closed-loop strategies are divided into several groups, such as stabilization to the manifold [49], [50], time-varying controllers [10], [23], [32], [36], [45], discontinuous feedback controllers [5], [2] or a combination of more than two approaches in [40] and [23].

This paper is organized as follows. Section II illustrates theoretical design of the nonholonomic manipulator. After introducing the nonholonomic gear in Section II-A, joint driving mechanisms are presented in Section II-B. Section II-C shows the nonlinear kinematic model of the nonholonomic manipulator. In Section III, it is shown that the kinematic model of the nonholonomic manipulator can be converted to the chained form. Mechanical design and prototyping are presented in Section IV. Various issues in mechanical design are discussed in Section IV-A. Section IV-B illustrates the analysis and computation of driving force of the nonholonomic gears toward practical applications. A prototype of the nonholonomic manipulator is introduced in Section IV-C. Some practical control schemes including both open-loop ones and feedback ones are proposed in Section V. Experimental results using the proposed control

Manuscript received December 4, 1999; revised August 11, 2000. This paper was recommended for publication by Associate Editor A. Bicchi and Editor A. De Luca upon evaluation of the reviewers' comments. This work was supported in part by NTT Company, Ltd., Japan Society of the Promotion of Science, the Center of Maritime Control Systems at NTH/SINTEF, and Ministry of Culture, Sports and Education under the Grant in Aid of Scientific Research (General Research (b)04452153). This paper was presented in part at the 1994 IEEE International Conference on Robotics and Automation, San Diego, CA, May 1994.

Y. Nakamura is with the Department of Mechano-Informatics, University of Tokyo, Tokyo 113, Japan (e-mail: nakamura@mech.t.u-tokyo.ac.jp).

W. Chung is with the Advanced Robotics Research Center, Korea Institute of Science and Technology, Seoul 136-791, Korea (e-mail: wjchung@kist-mail.kist.re.kr).

O. J. Sørdalen is with ABB Corporate Research, N-1375 Billingstad, Norway (e-mail: ole.j.soerdalen@no.abb.com).

Publisher Item Identifier S 1042-296x(01)02771-X.

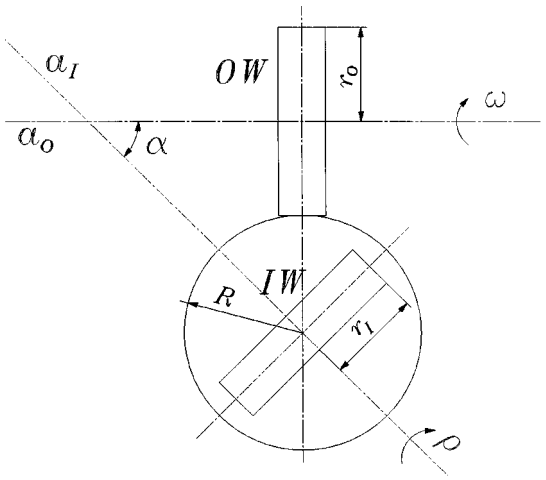

Fig. 1. Illustration of the nonholonomic gear seen from above.

schemes are presented with the fabricated prototype. Finally, some concluding remarks are given in Section VI.

II. Design of the Nonholonomic Manipulator

A. Nonholonomic Gear

Nonholonomic constraints of the wheeled mobile robots are due to the rolling contacts between tires and the ground. To drive passive joints exploiting nonholonomic constraints, it is needed to contrive some nonlinear mechanical elements inside the robot manipulator. In order to transmit velocities, we design a gear as illustrated in Fig. 1.

The basic components of this gear are a ball with radius R and two wheels IW and OW, indicating input wheel and output wheel, with radii r_{I} and r_{O}. The velocity constraints of the ball are only due to point contacts with the wheels. Wheel IW rotates about a fixed axis a_{I} with a given angular velocity ρ which makes the ball rotate. Point contact without slipping is assumed between wheel IW and the ball. Wheel OW is driven by the ball and rotates about an axis a_{O}. Wheel IW is in contact with the ball at the north pole, while wheel OW is on the equator such that its axis a_{O} lies in the plane of the equator. The angle between a_{I} and a_{O} is denoted by α.

When a ball and a wheel make a contact and rotate without slipping, the rolling-without-slipping constraint is not sufficient to uniquely determine the rotation of the ball. The rotation of the ball has two degrees of freedom, and the axis of rotation of the ball can lie in a plane involving the wheel axis and center of the ball. We call such a plane a constraint plane. If the ball makes contact with two wheels with different constraint planes, the rotation of the ball has only one degree of freedom. When the axes of the wheels are fixed, the ball rotates about the intersection of the two constraint planes. At this configuration, the ball rotates about axis A, which is parallel to a_{I} and passes through the center. When wheel IW rotates with ρ, the angular velocity Ω of the ball about axis A is given by

$$\Omega = -\frac{r_{\mathrm{I}}}{R}\rho. \tag{1}$$

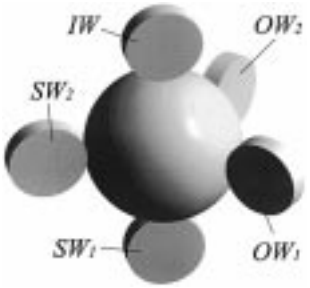

Fig. 2. Nonholonomic gear at joint i with supporting wheels.

The angular velocity ω of wheel OW is then given by

$$\omega = -\Omega\frac{R}{r_{\mathrm{O}}}\cos\alpha. \tag{2}$$

Combining (1) and (2) yields

$$\omega = \rho\frac{r_{\mathrm{I}}}{r_{\mathrm{O}}}\cos\alpha. \tag{3}$$

In addition to these three main components, additional supporting mechanisms are needed to maintain the contact between the ball and the wheels, and to assure the rotation of the ball. The analysis of constraint planes provides a suggestion to design supporting mechanism of the ball. The mechanism should support the ball without adding further constraints. A wheel that shares the constraint plane with OW, for example, adds no additional constraints as long as its axis does not move relative to the axis of OW. Therefore, we can add any number of wheels on the equator by fixing their axes to the constraint plane of OW and to the axis of OW. This fact implies a nonholonomic gear can have multiple OWs. Similarly, a wheel that shares the constraint plane with IW, located on the south pole can be added.

Fig. 2 shows a three-dimensional view of a nonholonomic gear at joint i with supporting wheels. SW indicates Supporting Wheel. The rotation axes of IW and SW_1 are fixed to link $i-1$. The rotation axes of OW_1, OW_2, and SW_2 are fixed to link i. Therefore, the nonholonomic gear in Fig. 2 consists of an input wheel IW, two output wheels OW_1 and OW_2, and two supporting wheels SW_1 and SW_2. Suppose that OW_2 in Fig. 2 corresponds to OW in Fig. 1. By the similar kinematic analysis, it is clear that the angular velocity of OW_1 in Fig. 2 is given by the following equation:

$$\omega = \rho\frac{r_{\mathrm{I}}}{r_{\mathrm{O}}}\sin\alpha \tag{4}$$

where α corresponds to the angle of joint i. From (3) and (4), it is obvious that the nonholonomic gear is a continuously variable transmission (CVT) which consists of single input and multiple output wheels. By changing the roles of input and output wheels, the gear ratios are functions of $1/\cos\alpha$ or $1/\sin\alpha$. Therefore, gear ratios of the nonholonomic gear are represented by trigonometric functions.

When α in (3) changes, wheels OW_1, OW_2, SW_2, and the ball rotate about the axis connecting the two poles. Even if $\dot{\alpha}$ is nonzero, the axis of rotation of the ball is axis A with respect to the coordinate frame fixed to link i, therefore (3) and (4) are still valid.

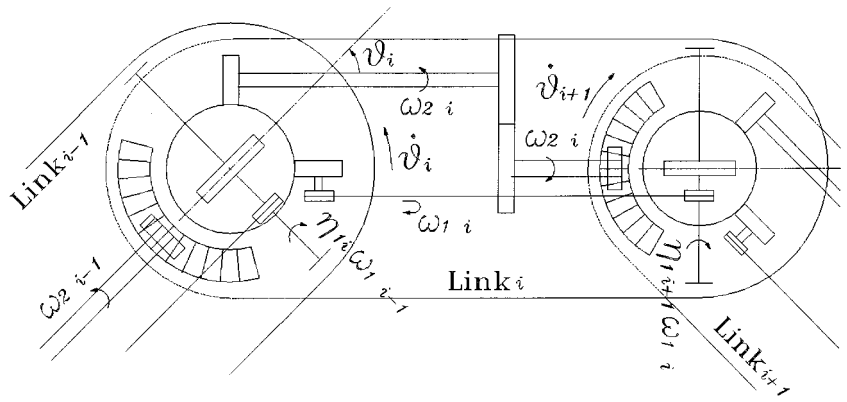

Fig. 3. The placement of the nonholonomic gear at joint $i-1$.

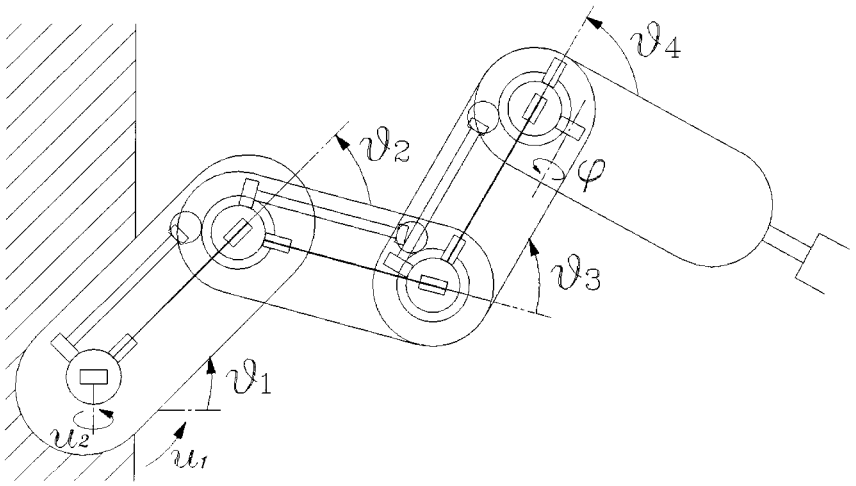

Fig. 4. Illustration of a four-joint manipulator and the velocity transmissions.

B. Joint Driving of the Nonholonomic Manipulator

Assume that the gear presented in the previous section is located at joint 1. We use one input wheel IW_1 and two output wheels, $\mathrm{OW}_{1,1}$ and $\mathrm{OW}_{2,1}$ where the last index indicates the joint. Notice that the nonholonomic gear is used as a velocity transmission which consists of single input and multiple output wheels. Fix axis $a_{\mathrm{I},1}$ of IW_1 to the base and the two axes of $\mathrm{OW}_{1,1}$ and $\mathrm{OW}_{2,1}$ to link 1 with orientations $\alpha_{1,1} \equiv \theta_1$ and $\alpha_{2,1} \equiv \theta_1 - \pi/2$ with respect to axis $a_{\mathrm{I},1}$. We denote the angular velocities of $\mathrm{OW}_{1,1}$ and $\mathrm{OW}_{2,1}$ by $\omega_{1,1}$ and $\omega_{2,1}$, respectively. Let the inputs u_1 and u_2 be the angular velocities of joint 1 and the input wheel IW_1 as follows:

$$\dot{\theta}_1 = u_1 \qquad \rho_1 = u_2. \tag{5}$$

By using mechanical transmissions, e.g., shafts and gears or belts and pulleys, $\mathrm{OW}_{2,1}$ drives the second joint as

$$\dot{\theta}_2 = \eta_{2,2} \qquad \omega_{2,1} = \eta_{2,2} \frac{r_{\mathrm{I},1}}{r_{\mathrm{O},1}} \sin\theta_1 \rho_1$$

since $\alpha_{2,1} = \theta_1 - (\pi/2)$ where $\eta_{2,2}$ is a gear ratio. We assume that $\mathrm{OW}_{1,1}$ and $\mathrm{OW}_{2,1}$ have the same radius $r_{\mathrm{O},1}$ for simplicity. Locate another similar gear at joint 2. By using mechanical transmissions from wheel $\mathrm{OW}_{1,1}$, let the angular velocity ρ_2 of IW_2 be given by

$$\rho_2 = \eta_{1,2} \qquad \omega_{1,1} = \eta_{1,2} \frac{r_{\mathrm{I},1}}{r_{\mathrm{O},1}} \cos\theta_1 \rho_1$$

since $\alpha_{1,1} = \theta_1$ where $\eta_{1,2}$ is a gear ratio. By locating such a gear at each joint i for $i \in \{1, \ldots, n-2\}$, we get

$$\dot{\theta}_{i+1} = \eta_{2,i+1} \frac{r_{\mathrm{I},i}}{r_{\mathrm{O},i}} \sin\theta_i \rho_i \tag{6}$$

$$\rho_{i+1} = \eta_{1,i+1} \frac{r_{\mathrm{I},i}}{r_{\mathrm{O},i}} \cos\theta_i \rho_i. \tag{7}$$

The coupling between the consecutive joints is illustrated in Fig. 3.

An example of four-joint planar nonholonomic manipulator is illustrated in Fig. 4.

The direction of the axis of a revolute joint $i+1$ can be arbitrary with respect to the axis of a joint i by designing the mechanical transmissions between the joints appropriately. Therefore, the manipulator is not restricted to be planar.

C. Kinematic Model of the Nonholonomic Manipulator

In addition to the joint angles, the orientation of one of the OWs at joint $n-1$, which is denoted by φ, is added to the kinematic model. By taking φ as a control parameter, kinematic

model of the nonholonomic manipulator can be converted to the chained form. Notice that φ is not a control input and the details of φ will be presented in Section V. Accordingly, there are $n-1$ joints for an n-dimensional kinematic model.

From (5)–(7) and adding φ, the following kinematic model in the configuration space S^n is obtained:

$$\dot{\theta}_1 = u_1 \tag{8}$$

$$\dot{\theta}_i = k_i \sin\theta_{i-1} \prod_{j=1}^{i-2} \cos\theta_j u_2, \qquad i \in \{2, \ldots, n-1\} \tag{9}$$

$$\dot{\varphi} = k_n \prod_{j=1}^{n-1} \cos\theta_j u_2 \tag{10}$$

where

$$k_i \triangleq \eta_{2,i} \prod_{j=1}^{i-1} \eta_{1,j} \frac{r_{\mathrm{I},j}}{r_{\mathrm{O},j}} \qquad k_n \triangleq \prod_{j=1}^{n-1} \eta_{1,j} \frac{r_{\mathrm{I},j}}{r_{\mathrm{O},j}} \tag{11}$$

where $\eta_{1,1} = 1$.

It is noteworthy that this kinematic model has a similar structure as the kinematic model of a car with $n-3$ trailers, but not identical. The angle θ_1 can be thought of as the steering angle and θ_{n-1} and φ can be thought of as the y- and x-position, respectively, of the last trailer.

The system's nonholonomic constraints are due to the rolling contact between the balls and the wheels. The $n-2$ constraints in the joint space are given from (8)–(10) by

$$k_i \sin\theta_{i-1}\dot{\varphi} - k_n \prod_{j=i-1}^{n-1} \cos\theta_j \dot{\theta}_i = 0, \qquad i \in \{2, \ldots, n-1\}. \tag{12}$$

An alternative formulation of the kinematics (8)–(10) is

$$\dot{\theta}_1 = u_1 \tag{13}$$

$$\dot{\theta}_i = k_i \sin\theta_{i-1} v_{i-1}, \qquad i \in \{2, \ldots, n-1\}$$

$$\dot{\varphi} = k_n \cos\theta_{n-1} v_{n-1} \tag{14}$$

where

$$v_{i-1} = \prod_{j=1}^{i-2} \cos\theta_j u_2 = C_1^{i-2}(\Theta_{i-2}) u_2$$

where $\Theta_{i-2} \triangleq [\theta_1, \ldots, \theta_{i-2}]^{\mathrm{T}}$ and

$$C_1^{i-2}(\Theta_{i-2}) \triangleq \prod_{j=1}^{i-2} \cos\theta_j.$$

By setting configuration variables $\xi \triangleq [\theta_1, \ldots, \theta_{n-1}, \varphi]^{\mathrm{T}}$, the kinematic model can be represented using input vectors as the following equations:

$$\dot{\xi} = \boldsymbol{V}_1 u_2 + \boldsymbol{\Omega}_1 u_1 \tag{15}$$

$$\boldsymbol{V_1} = [0, k_2 s_1, k_3 s_2 C_1^1, \ldots, k_{n-1} s_{n-2} C_1^{n-3}, k_n c_{n-1} C_1^{n-2}]^{\mathrm{T}} \tag{16}$$

$$\boldsymbol{\Omega_1} = [1, 0, \ldots, 0]^{\mathrm{T}} \tag{17}$$

where $s_i \triangleq \sin\theta_i$ and $c_i \triangleq \cos\theta_i$.

III. Conversion to the Chained Form

A. Triangular Structure and Chained-Form Conversion

In order to control the nonholonomic manipulator, the kinematic model (8)–(10) will be converted into a chained form implying that existing control laws for chained form can be applied. Conversion of the kinematic model of a car with n trailers into a chained form was presented in [37] and an exponentially convergent stabilizer was proposed in [39]. Chained form was introduced in [26]. The chained form considered here is given by

$$\dot{z}_1 = v_1 \tag{18}$$

$$\dot{z}_2 = v_2 \tag{19}$$

$$\dot{z}_i = z_{i-1} v_1, \qquad i \in \{3, \ldots, n\}. \tag{20}$$

To convert the kinematic model into a chained form, we present the following theorem on the conversion of triangular systems into a chained form. First, denote

$$\underline{x}_i \triangleq [x_i, \ldots, x_n]^{\mathrm{T}}$$

$$\underline{f}_i(\underline{x}_{i-1}) \triangleq [f_i(\underline{x}_{i-1}), \ldots, f_n(\underline{x}_{n-1})]^{\mathrm{T}}.$$

Theorem 1: Let a driftless, two-input system be given by

$$\dot{x}_1 = u_1 \tag{21}$$

$$\dot{x}_2 = u_2 \tag{22}$$

$$\dot{x}_i = f_i(\underline{x}_{i-1}) u_1, \qquad i \in \{3, \ldots, n\} \tag{23}$$

where $f_i(\cdot)$ is a smooth function. Assume that at a configuration $x = p$ on the configuration manifold

$$\left.\frac{\partial f_i(\underline{x}_{i-1})}{\partial x_{i-1}}\right|_{x=p} \neq 0 \qquad \forall i \in \{3, \ldots, n\}. \tag{24}$$

Then, a coordinate transformation $z = h(x)$ and an input feedback transformation $v = g(x)u$ converting (21)–(23) into the chained form in (18)–(20) in a neighborhood of $x = p$ is given by

$$z_n = h_n(x_n) \tag{25}$$

$$z_i = h_i(\underline{x}_i) \triangleq \frac{\partial h_{i+1}(\underline{x}_{i+1})}{\partial \underline{x}_{i+1}} \underline{f}_{i+1}(\underline{x}_i) \tag{26}$$

$$z_1 = h_1(x_1) \triangleq x_1 \tag{27}$$

where $i \in \{2, \ldots, n-1\}$ and $h_n(x_n)$ is any smooth function such that

$$\left.\frac{\partial h_n(x_n)}{\partial x_n}\right|_{x=p} \neq 0$$

and

$$v_1 = u_1 \tag{28}$$

$$v_2 = \frac{\partial h_2(\underline{x}_2)}{\partial \underline{x}_3} \underline{f}_3(\underline{x}_2) u_1 + \frac{\partial h_2(\underline{x}_2)}{\partial x_2} u_2. \tag{29}$$

Proof: Proof is given in [42].

B. Chained-Form Conversion of the Nonholonomic Manipulator

The kinematic model of the nonholonomic manipulator (8)–(10) can be represented locally by the following form:

$$\dot{\theta}_1 = u_1 \tag{30}$$

$$\dot{\varphi} = \mu_2 \tag{31}$$

$$\dot{\theta}_i = k_i \tan\theta_{i-1} \frac{1}{k_n \prod_{j=i}^{n-1} \cos\theta_j} \mu_2, \qquad i \in \{2, \ldots, n-1\} \tag{32}$$

$$\mu_2 \triangleq k_n \prod_{j=1}^{n-1} \cos\theta_j u_2.$$

This system has the structure as given by (23). From Theorem 1, it follows that (8)–(10) is convertible to a chained form.

Corollary 1: The kinematic model in (8)–(10) is convertible into chained form in the subspace $\theta_i \in (-(\pi/2), (\pi/2))$, $i \in \{1, \ldots, n-1\}$. A coordinate transformation and an input feedback transformation is given by (25)–(29) with $x = [\varphi, \theta_1, \theta_2, \ldots, \theta_{n-1}]^{\mathrm{T}}$ and

$$f_{i+1}(\underline{x}_i) = k_i \tan\theta_{i-1} \frac{1}{k_n \prod_{j=i}^{n-1} \cos\theta_j}.$$

Proof: The modified kinematic model in (30)–(32) is valid for $\theta_i \in (-(\pi/2), (\pi/2))$ where $i \in \{1, \ldots, n-1\}$. The result then follows readily from Theorem 1 and (30)–(32) since for $\theta_{i-1} \in (-(\pi/2), (\pi/2))$ and for all $i \in \{2, \ldots, n-1\}$

$$\frac{\partial f_{i+1}(\underline{x}_i)}{\partial x_i} = k_i \frac{1}{\cos^2\theta_{i-1}} \neq 0.$$

□

It can be easily checked that the kinematic model in (30)–(32) cannot be converted to the chained form without a control parameter φ. Although it has a triangular structure as in (21)–(23), the condition in (24) cannot be satisfied. Furthermore, φ plays a significant role in controller design, which will be discussed in Section V-C.

IV. Prototyping of the Nonholonomic Manipulator

A. Issues in Mechanical Design

Since a nonholonomic manipulator was theoretically designed from the viewpoint of kinematic constraints and nonlinear control, mechanical implementation and prototyping are significant in practice. A prototype should be carefully designed to assure the principle of velocity transmission.

In order to assure frictional force at a contact zone, appropriate surface normal forces should be applied at the contact zone between a ball and wheels. Two cantilever springs, which make the mechanical structure simple, are employed at each nonholonomic gear. One is for the supporting (not the input) wheel at the south pole, and the other is for the supporting (not the output) wheel at the equator. Locations of wheels of the prototype are same as those in Fig. 2. In Fig. 5, a supporting wheel with a cantilever spring is presented.

The cantilever spring drawn with dotted line represents its original shape. By inserting a spacer (a piece of metal slice) whose thickness is equal to δ, surface normal force is generated. A cantilever spring drawn with solid line represents its deformed shape. Since a spring force is proportional to the deflection, once we have prepared several thicknesses of spacers, then, by choosing many different combinations, the spring force can be widely changed.

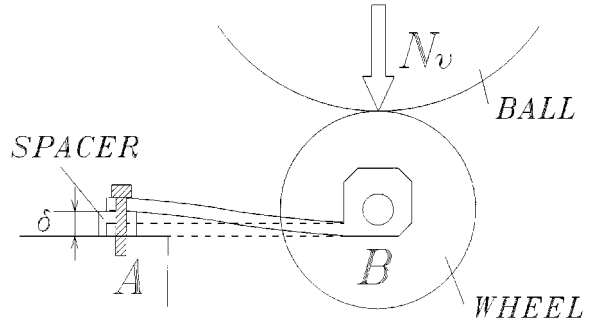

Fig. 5. A supporting wheel with a cantilever spring.

Machining errors of mechanical components might cause a difference between the real deflection and the predicted one. To set an accurate spring force, strain gauges were attached to each cantilever and calibrations were carried out. Resultant spring forces can be adjusted from the strain gauge signal after constructing all the mechanical components.

B. Analysis and Computation of Driving Force

In order to transmit angular velocity by friction drive, large frictional forces are desirable between two rotating bodies. Frictional force depends on the surface normal force and a coefficient of friction. The nominal value of a coefficient of friction is determined by material property. Although surfaces can be made rough by sand blasting, its effect on a coefficient of friction is not much under the high pressure. However, applying too large surface normal forces cause yielding and plastic deformation of materials.

The general solution to the contact problem of two elastic solids is as well known as the Hertz theory of elastic contact. Some useful results can be found in the literature [48], [43], [12].

For the prototype nonholonomic manipulator designed, radii of a ball and a wheel are 19 and 10 mm. Considering these conditions, the maximum shear stress is presented as a function of the applied normal force in Fig. 6.

The shear strength of material used (steel SUJ2) is approximately 700 $\mathrm{N/mm^2}$. The frictional coefficient was assumed to be 0.1. From Fig. 6, we conservatively see that we can apply up to 120 N of surface normal force using a cantilever spring.

C. Prototype of the Nonholonomic Manipulator

According to the design concept presented in previous sections, a prototype of the nonholonomic manipulator was fabricated as shown in Fig. 7. The prototype has four revolute joints, whose kinematic model corresponds to five-dimensional chained form, as illustrated in Section II-C. It is a planar structure to avoid te problems due to the lack of actuating torques to support the gravity. If sufficient joint actuating torques can be obtained, it can be designed with a spatial structure having arbitrary directions of joint axes.

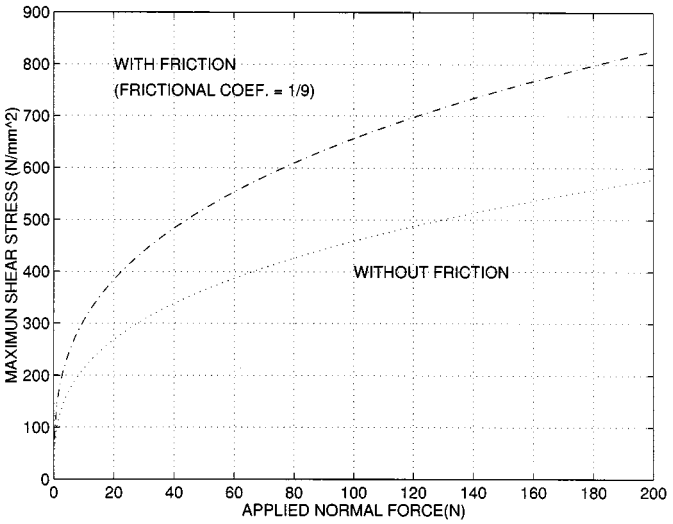

Fig. 6. Applied normal force versus maximum shear stress.

Fig. 7. Prototype of the nonholonomic manipulator.

There are two actuators in total and both are located at the base. There are many possible alternatives in determining the location of actuators. Putting actuators on the base is desirable because there are only passive mechanical components on the robot arm, which results in light weight and simple structure of the arm. Fig. 8 shows the nonholonomic gear at the second joint.

V. Control of the Nonholonomic Manipulator

There are two major streams in control of nonholonomic systems. One is open-loop motion planning and the other is feedback control. Control inputs can be easily computed by applying the open-loop strategies, which provide simple and practical solutions in many cases. However, an open-loop controller cannot deal with uncertainties and disturbances. Feedback controllers show complementary advantages and disadvantages of the open-loop controllers. Detailed explanations are given in [8].

In this section, one open-loop and two feedback controllers are experimentally tested. The first approach is to employ time polynomial inputs in [47]. The second is the feedback control with exponential convergence in [39]. The first and the second experiments show that any of the previously proposed

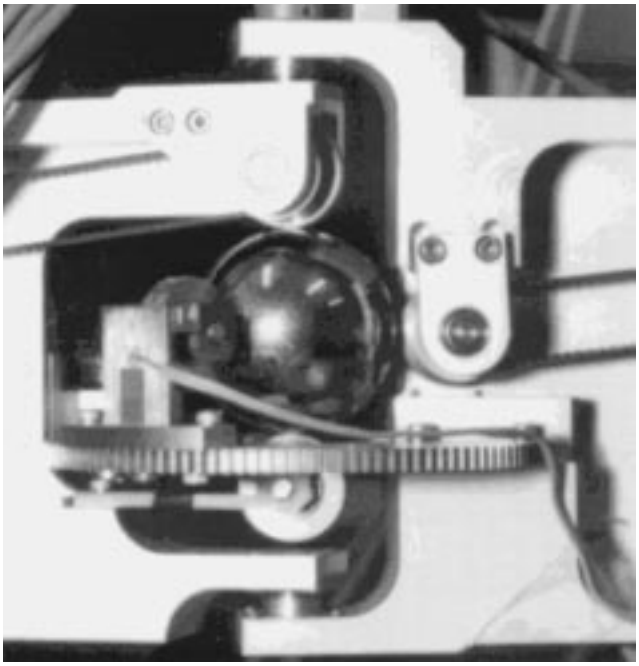

Fig. 8. Prototype of the nonholonomic gear.

controllers to the chained form can be applied to control the nonholonomic manipulator. Finally, the feedback control by pseudolinearization is proposed in order to provide a practical control solution of the nonholonomic manipulator.

In simulations and experiments, control schemes are applied to the three-joint manipulator model as shown in Fig. 9. Correspondence of simulations and experiments in this section is presented in Table I.

For the four-joint model, some mathematical and mechanical problems were faced. Although there is no limitation on the number of the controllable joint, a kinematic model becomes ill-conditioned as the number of the joint increases. This problem is further discussed in [7]. Therefore, the scope of experiments will be limited to the three-joint model, which corresponds to the four-dimensional chained-form system. φ, which is a rotation angle of the OW of the third joint, is a control parameter and free boundary conditions can be given.

A. Open-Loop Control

There are many existing open-loop controllers to the chained form. Sinusoidal inputs [26], [47], time polynomial inputs [47], and piecewise constant inputs [24] are typical examples. Such control schemes are common in that inputs are given by solving algebraic equations using the input parameterization. Any of such control laws can be applied to control the nonholonomic manipulator. In this section, time polynomial inputs are applied because inputs are easily obtained by solving simple algebraic equations and resultant trajectories are smooth.

The inputs to the chained form in (18)–(20) are given by time polynomials as follows:

$$v_1 = b_0 \tag{33}$$

$$v_2 = c_0 + c_1 t + \cdots + c_{n-2} t^{n-2}. \tag{34}$$

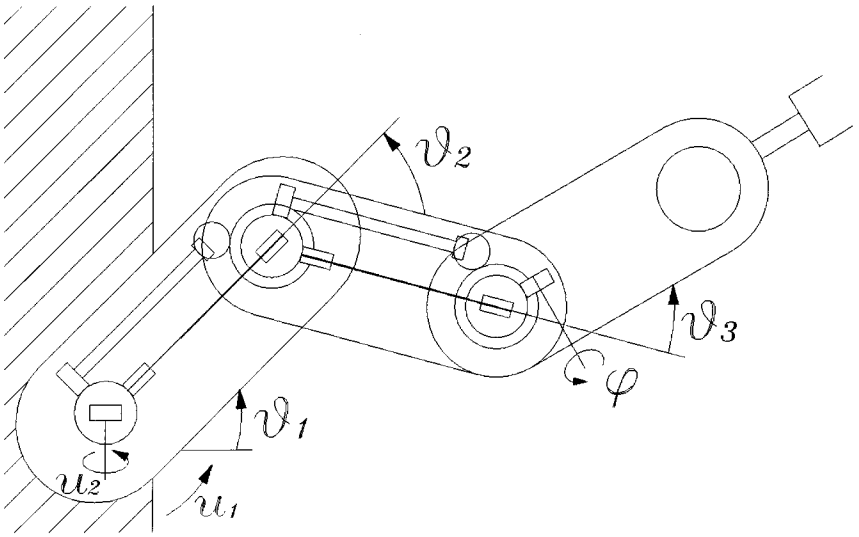

Fig. 9. The four-dimensional nonholonomic manipulator consists of three joints.

TABLE I
CORRESPONDENCE OF SIMULATIONS AND EXPERIMENTS FOR THE NONHOLONOMIC MANIPULATOR

Simulation 1	no experiment
Simulation 1 modified by time scaling	Experiment A
Simulation 3	Experiment B
Simulation 4	Experiment C

To steer the state z from $z(0)$ to $z(T)$ in the finite time T, assuming that $z_1(0) \neq z_1(T)$, the coefficients are given as follows:

$$b_0 = \frac{z_1(T) - z_1(0)}{T}$$

$$M \begin{bmatrix} c_0 \\ c_1 \\ \vdots \\ c_{n-2} \end{bmatrix} + N \begin{bmatrix} z_2(0) \\ z_3(0) \\ \vdots \\ z_n(0) \end{bmatrix} = \begin{bmatrix} z_2(T) \\ z_3(T) \\ \vdots \\ z_n(T) \end{bmatrix}$$

where

$$M_{i,j} \triangleq \frac{{b_0}^{i-1}(j-1)!}{(i+j-1)!} T^{i+j-1}$$

$$N_{i,j} \triangleq \left\{ \begin{array}{ll} 0, & i < j \\ \dfrac{{b_0}^{i-j}}{(i-j)!} T^{i-j}, & i \geq j \end{array} \right\}.$$

If $z_1(0) \neq z_1(T)$, M is nonsingular. Since free boundary conditions can be given to z_1, M can always be made nonsingular.

The joint and motor trajectories are computed. In Fig. 10, joint angles versus time angles are plotted (simulation 1). Fig. 11 shows input angular velocities of two actuators. Manipulator motions in $\mathbb{R}^2$ are shown in Fig. 12. Fig. 13 shows the motion with respect to time which corresponds to z axis. The total time T was set to 10 s. The gear ratios were selected as $[k_2, k_3] = [1/10, 1/10]$ which are the same as the prototype. Joint angles of initial configuration $\theta(0)$ and desired configuration θ_d are $\theta(0) = [-20°, -20°, -20°]$, $\theta_{\rm d} = [20°, 20°, 20°]$.

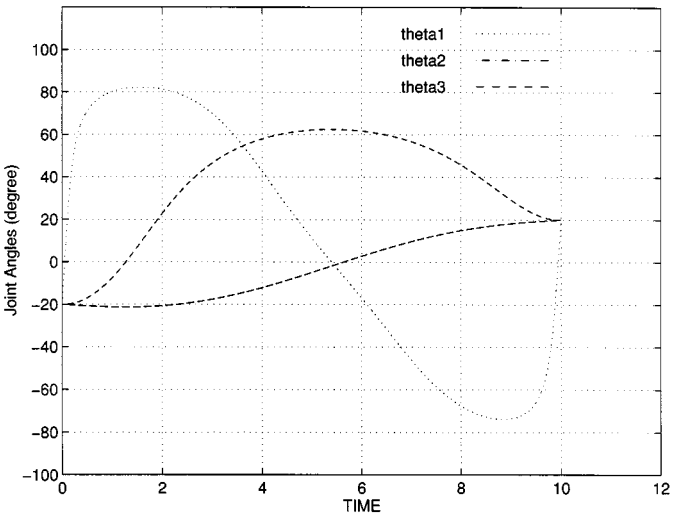

Fig. 10. Joint angles versus time with polynomial inputs: simulation 1.

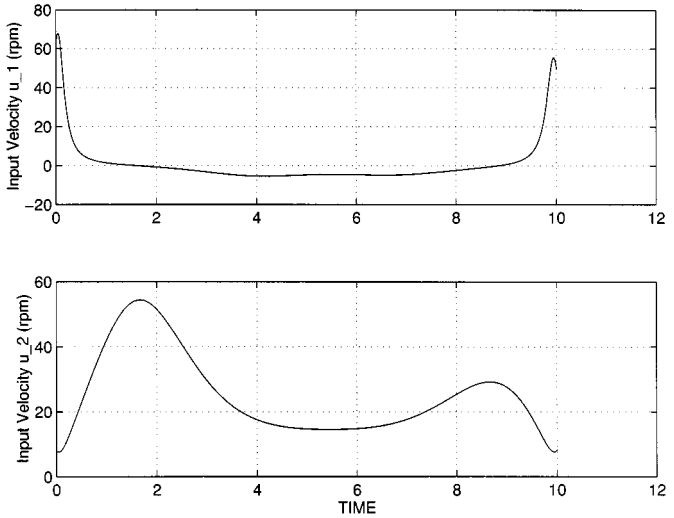

Fig. 11. Input angular velocities versus time with polynomial inputs simulation 1.

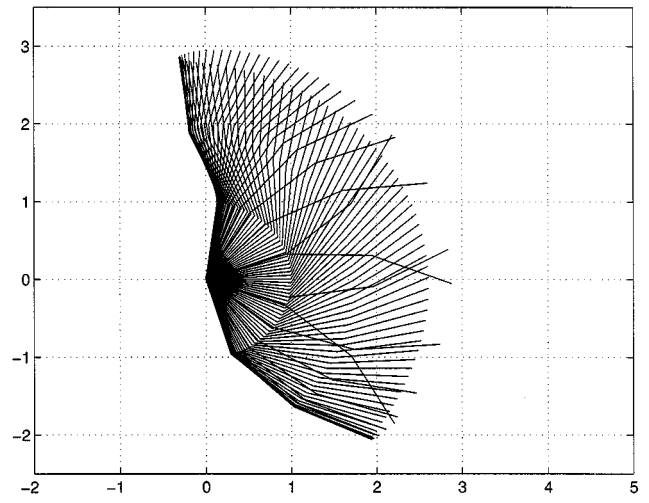

Fig. 12. Manipulator motion in $\mathbb{R}^2$ with polynomial inputs: simulation 1.

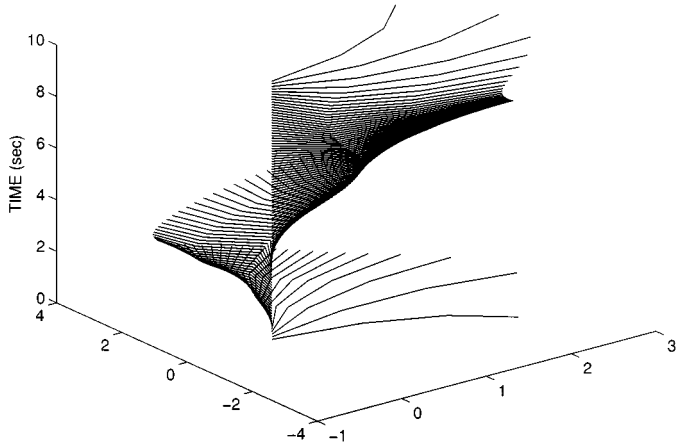

Fig. 13. Manipulator motion in $\mathbb{R} \times t$ with polynomial inputs: simulation 1.

From Fig. 10, it is clear that the joint angles reach their desired values.

Although motions are successfully planned in simulations, the nonholonomic manipulator has mechanical limitations in practice. Trajectories are physically infeasible because of actuator saturations or high joint accelerations exceeding the limitations of nonholonomic gears.

A time scaling is a powerful tool to deal with this problem. Suppose that a new time scale $\hat{t}$ is given as a following equation:

$$\hat{t} = S_{\mathrm{f}} t \tag{35}$$

where S_{f} is a scaling factor which is assumed to be a constant during a time interval $[0, t]$. From (12), it is obvious that the scaling factor S_{f} does not appear in the constraint (35) after time scaling. Equation (15) can be simply rewritten as $\dot{\xi} = g(\xi)u$. Since $d\hat{t} = S_{\mathrm{f}} dt$, the following equation is obtained:

$$\frac{d\hat{\xi}}{d\hat{t}} = g(\hat{\xi})\frac{1}{S_{\mathrm{f}}}u = g(\hat{\xi})\hat{u} \tag{36}$$

where $\hat{\xi}$ and $\hat{u}$ are scaled coordinates and inputs, respectively. Since $\hat{u} = 1/S_{\mathrm{f}} u$ from (36), it is clear that the time scaling of the nonholonomic manipulator implies the scaling of inputs. Since $\xi(t) = \hat{\xi}(S_f t) = \hat{\xi}(\hat{t})$, trajectories in the joint space do not change. Therefore, time scaling can be applied to plan a physically feasible path for any open-loop controller. Another expression of time scaling can be found in [41] for the polynomial inputs.

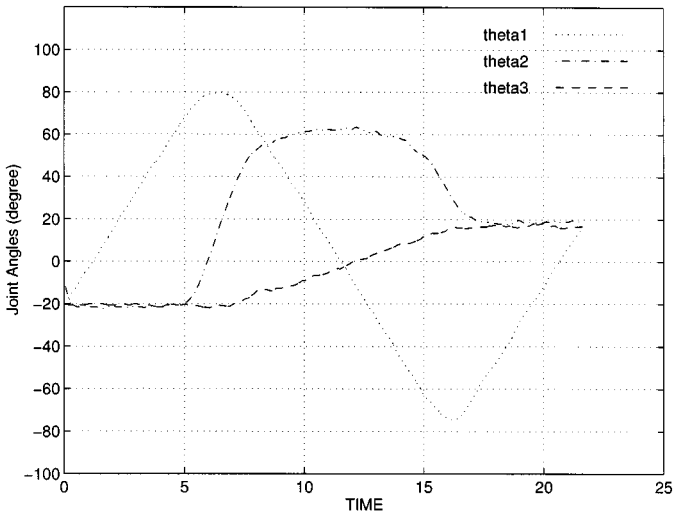

Fig. 14. Experimented joint angles versus time with time scaled polynomial inputs: experiment A.

Here, time scaling is applied to saturate an input angular velocity u_1, i.e.,

$$u_1 = \mathrm{sat}(u_1, u_{1,\mathrm{sat}}) \tag{37}$$

where

$$\mathrm{sat}(p, K) \triangleq \begin{cases} p, & |p| < K \\ K\mathrm{sgn}(p), & |p| \geq K. \end{cases}$$

The velocity limit of u_1 is set first, and trajectories computed by time polynomial inputs are modified by time scaling. The computed motion was experimentally tested by applying velocity control to two motors for their predetermined trajectories (experiment A). Fig. 14 illustrates the joint trajectories of experiment. The index of error of the joint angles is defined as follows:

$$E = \sum_{i=1}^{3} |\theta_{i,\mathrm{f}} - \theta_{i,\mathrm{d}}| \tag{38}$$

where $\theta_{i,\mathrm{f}}$ is a joint angle after completing control, $\theta_{i,\mathrm{d}}$ is a desired joint angle. At the end of experiment A, E was $5°$. The backlash at the spur gear and the low stiffness of the long shaft would have caused error.

Measured input velocities are plotted in Fig. 15. The absolute value of the desired velocity limit of $u_{1,\mathrm{sat}}$ was selected as $0.3141\ (\mathrm{rad/sec}) = 3\ (\mathrm{r/min})$. The total time needed to reach the goal was 22 s, it was 12 s longer than the case of the standard time polynomial inputs.

B. Feedback Control with Exponential Convergence

Feedback control would be significant to deal with various uncertainties. Feedback control of a class of systems, including driftless nonholonomic systems is known to be difficult because of the limitations which were pointed out by the Brockett's theorem [3], i.e., there is no smooth, static state feedback law that asymptotically stabilizes the system to a given configuration.

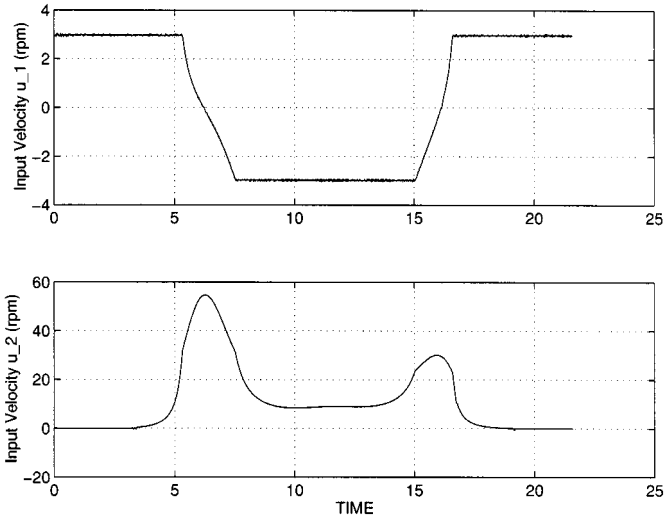

Fig. 15. Experimented input angular velocities of two motors versus time with time scaled polynomial input: experiment A.

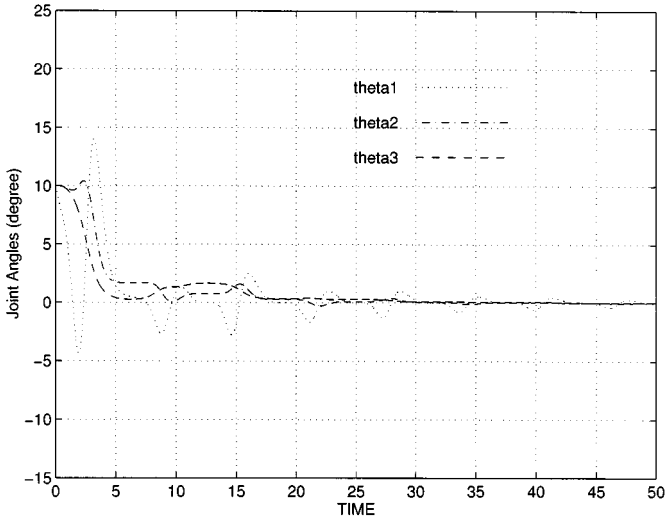

Fig. 16. Joint angles versus time with the exponentially convergent feedback law: simulation 3.

Therefore, many approaches were made without violating the Brockett's necessary conditions. Typical examples are time-dependent feedback law by Samson [36] or Pomet [32]. Since these controllers are smooth, convergence rate is slow [14].

In this section, the strategy from [38] and [39] resulting in a feedback control with exponential convergence is applied. The control scheme is piecewise continuous and time dependent. The feedback control is given by the following equations:

$$v_1 = \gamma(z(t_i))\, l(t) \tag{39}$$

$$v_2 = -\lambda_2(z_2 - z_2^{\mathrm{d}}) + \dot{z}_2^{\mathrm{d}} \tag{40}$$

$$z_2^d \triangleq (-\lambda_3(z_3 - z_3^{\mathrm{d}}) + \dot{z}_3^{\mathrm{d}})/\gamma$$

$$z_3^{\mathrm{d}} \triangleq (-\lambda_4 z_4)/\gamma$$

where $l(t) = (1 - \cos\omega t)/2$. $\omega = 2\pi/T$ and $T = t_{i+1} - t_i$ are supposed to be constants. The parameter $\gamma(\cdot)$ is given as follows:

$$\gamma = \mathrm{sat}(-[z_1(t_i) + \mathrm{sgn}(z_1(t_i))G(\|q(t_i)\|)]\beta, K) \tag{41}$$

where $q = [z_2, \ldots, z_n]^{\mathrm{T}}$ and

$$G(\|q(t_i)\|) \triangleq \kappa \|q(t_i)\|^{1/2(n-2)} \tag{42}$$

$$\beta \triangleq \frac{1}{\int_{t_i}^{t_{i+1}} l(\tau)d\tau} \tag{43}$$

$$\mathrm{sgn}(p) = \begin{cases} 1, & p \geq 0 \\ -1, & p < 0 \end{cases} \tag{44}$$

where κ is a positive constant.

In the simulation (simulation 3), the series of time t_i form the set $\{0, 2\pi, 4\pi, 6\pi, \ldots\}$, i.e., $\omega = 1$, where t_0 is zero. The controller parameters were chosen as follows: $\lambda_2 = \lambda_3 = \lambda_4 = 0.5$, $\kappa = 1.5$, and $K = 10$.

In Fig. 16, simulated joint angles are plotted (simulation 3). The initial configuration $\theta(0)$ and the desired configuration θ_{d} are $\theta(0) = [10°, 10°, 10°]$, $\theta_d = [0°, 0°, 0°]$. From Fig. 16, it is clear that joint angles converge to the origin with exponential convergence.

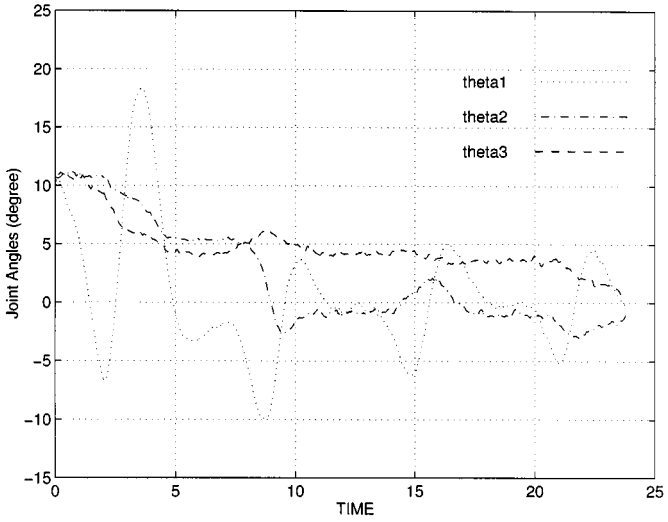

Fig. 17. Joint angles versus time with the exponential convergent feedback law: experiment B.

An experiment was carried out under the same condition (experiment B). Fig. 17 shows the result. We set the condition of terminating the control as $E < 3°$ in (38). Profiles of the joint angle trajectories are similar to those of the first 23 s of Fig. 16. A small difference of the magnitude of oscillation might be due to the effect of joint backlashes, slippage at the nonholonomic gear, and so forth.

C. Feedback Control by Pseudolinearization

The main drawback of the feedback controller presented in the previous section is the frequent switching, which results in high energy and oscillatory motions. Furthermore, feedback laws become highly complicated as the dimension of system increases. In this section, a simple feedback strategy is developed toward practical implementations.

Setting $v_1 = a_0$ for the chained form of (18)–(20), the system is described as follows:

$$\dot{z_1}(t) = a_0 \tag{45}$$

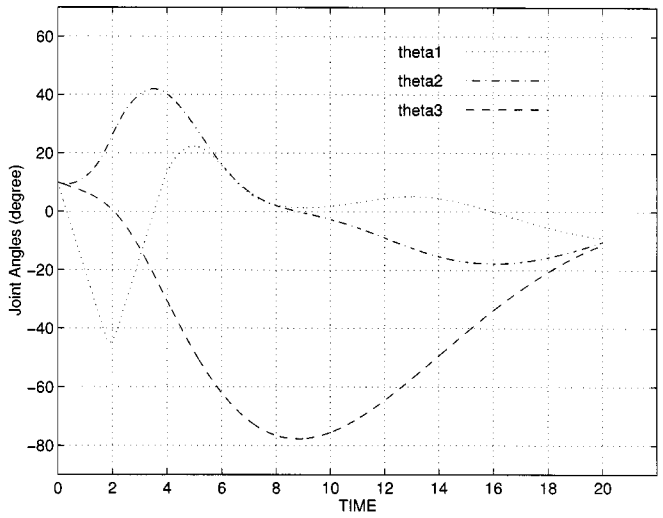

Fig. 18. Joint angles versus time with the feedback control by pseudolinearization: simulation 4.

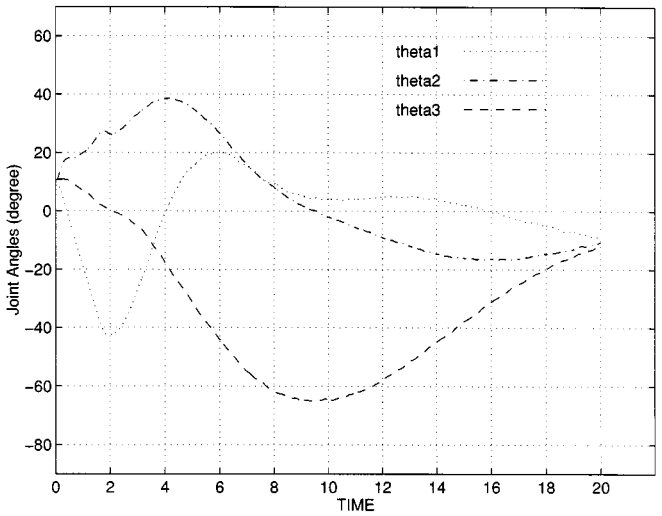

Fig. 19. Joint angles versus time with the feedback control by pseudolinearlization: expression C.

$$\begin{bmatrix} \dot{z}_2(t) \\ \dot{z}_3(t) \\ \vdots \\ \dot{z}_n(t) \end{bmatrix} = A \begin{bmatrix} z_2(t) \\ z_3(t) \\ \vdots \\ z_n(l) \end{bmatrix} + \begin{bmatrix} 1 \\ 0 \\ \vdots \\ 0 \end{bmatrix} v_2 \tag{46}$$

$$A_{i.j} \triangleq \begin{cases} 0, & 1-j \neq 1 \\ a_0, & i-j=1. \end{cases}$$

Equation (46) is the state equation of a linear system. Therefore, we can apply linear control theory. z_1 in (45) is controlled with open loop. Since z_1 corresponds to parameter φ in Fig. 9, an arbitrary boundary condition of z_1 can be chosen.

It is not easy to stabilize the system of (46) to a nonzero desired configuration with the standard linear control theory. Fortunately, a nonlinear coordinate transformation of the chained system was developed in [42] as the follows:

$$z_i^r \triangleq z_i^{\mathrm{d}} + \sum_{j=2}^{i-1} z_j^{\mathrm{d}} \frac{1}{(i-j)!} (z_1 - z_1^{\mathrm{d}})^{i-j} \tag{47}$$

$$\bar{z}_i = z_i - z_i^r, \qquad i \in \{1, \ldots, n\} \tag{48}$$

where z_i^{d} is the desired point. This coordinate transformation is valid for any control strategy stabilizing the chained system to the origin. The equilibrium point of the closed-loop system is shifted to an arbitrary desired configuration z_i^{d}, using the transformation of (47) and (48). In order to use coordinate transformations of (47) and (48), $z_i (i \in \{1, \ldots, n\})$ should be stabilized to the origin. The pseudolinearized system of (46) can be stabilized to the origin by a simple state feedback. By setting a proper a_0, z_1 goes to 0 with linear convergence. This determines a finite time to control.

Fig. 18 plots joint angles versus time resulted from the feedback control by a pseudolinearization (simulation 4). The initial configuration $\theta(0)$ and the desired configuration θ_{d} are $\theta(0) = [10^\circ, 10^\circ, 10^\circ]$, $\theta_d = [-10^\circ, -10^\circ, -10^\circ]$. $v_1 (= a_0)$ was -0.3272 (rad/sec) and the finite time of convergence was 20 s. Feedback gains were $[g_1, g_2, g_3] = [3.7131, -5.7865, 3.1623]$. It is observed that the joint angles reach the desired values after the finite time.

An experiment was carried out under the same condition (experiment C). Fig. 19 shows experimental joint angles. The index of errors at the 20 s was $E = 1^\circ$. Profiles of the joint angles are similar to those of Fig. 18. Since the control scheme requires only simple computation, it can be used for a nonholonomic manipulator with large number of joints.

Similar approaches to the pseudolinearization were made previously. For example, Samson pointed out this idea in [36]. Sampei [34], [35] proposed a general formulation of pseudolinearization which can be extended to a class of driftless systems including chained form. Astolfi's controller [2] is designed based on the idea of uniform convergence of z_1.

However, the strategy introduced in this section is especially useful for the nonholonomic manipulator because z_1 is designed as a parameter, which cannot be achieved by the other systems. For an n-trailer system, z_1 corresponds to the x coordinate of the last trailer. Therefore, z_1 should be carefully dealt with. Convergence analysis of Sampei's controller was not clear because z_1 was controlled independently. For the nonholonomic manipulator, only a subsystem of (46) should be considered and its convergence rate is exponential.

VI. Conclusion

Using the nonholonomic gears introduced in this paper, the nonholonomic manipulator with n revolute joints is made completely controllable in T^n with only two actuators. For some applications, where only limited resources are available, it would be essential to reduce the number of actuators and to reduce the cost and weight without reducing the reachable configuration space.

This paper showed how a manipulator can be designed and controlled if it is preferred to have a few actuators. The basic idea is to introduce nonholonomic constraints in the design and exploit the property to increase the dimension of the reachable space. The nonholonomic gear was employed to build underactuated manipulators, but may be used in many other applications as a continuously variable transmission with a nonlinear gear ratio.

The nonholonomic manipulator was designed from the viewpoint of kinematics and velocity constraints. However, the practical control performance is dependent upon the system dynamics. If there exists discontinuity in the input angular velocity, the joint velocity becomes infeasible due to the violation of the kinematic constraints. The discontinuity of the joint velocity would require large joint torques exceeding the mechanical limitation of the nonholonomic gear. Therefore, the input of the nonholonomic manipulator should be continuous in order to guarantee kinematic constraints. Once a smooth manipulator motion is obtained, joint torques of the nonholonomic manipulator are computed by applying the conventional inverse dynamics. The maximum joint torque is limited by the frictional forces of the nonholonomic gear. Therefore, feasible manipulator motions should be carefully planned by taking the joint torque limitations into account.

To stabilize the system, it is designed with a triangular structure that is locally convertible into the chained form by a theorem presented in this paper. Existing open- and closed-loop controllers for the chained form can then be used to control the nonholonomic manipulator.

Since there are only two velocity inputs, the nonholonomic manipulator has only two degrees of freedom. Therefore, if exact tracking is required in the joint space of higher dimension, it is generally impossible. However, since the nonholonomic manipulator is controllable, any path in the n-dimensional joint space can be followed with any specified non-zero accuracy. Obstacles in the workspace can therefore be avoided.

Various issues in mechanical design of the nonholonomic manipulator were discussed. Analysis and computations for the mechanical design were carried out and used for the fabrication of the prototype.

By simulations and experiments, it was shown that any existing controllers of the chained form can be applied to control the nonholonomic manipulator. Experimental results proved the correctness of the nonholonomic manipulator design and the usefulness of the proposed control schemes. A time scaling technique was introduced to plan physically feasible paths. A practical feedback strategy by pseudolinearization was proposed for control simplicity.

ACKNOWLEDGMENT

The authors would like to acknowledge the reviewers of this paper for their valuable comments. W. Chung acknowledges the Pohang Steel Company Scholarship Society.

REFERENCES

[1] P. K. Agarwal, J. C. Latombe, R. Motwani, and P. Raghavan, "Nonholonomic path planning for pushing a disk among obstacles," in *Proc. 1997 IEEE Int. Conf. Robotics and Automation*, Albuquerque, NM, Apr. 1997, pp. 3124–3129.

[2] A. Astolfi, "Exponential stabilization of a car-like vehicle," in *Proc. 1995 IEEE Int. Conf. Robotics and Automation*, Nagoya, Japan, May 1995, pp. 1391–1396.

[3] R. W. Brockett, "Asymptotic stability and feedback stabilization," in *Differential Geometric Control Theory*, R. W. Brockett, R. S. Millman, and H. J. Sussman, Eds. Birkhauser, 1983, pp. 181–208.

[4] L. Bushnell, D. Tilbury, and S. Sastry, "Extended goursat normal forms with applications to nonholonomic motion planning," in *Proc. 32th Conf. Decision and Control*, San Antonio, TX, Dec. 1993, pp. 3447–3452.

[5] C. C. de Wit and O. J. Sørdalen, "Exponential stabilization of mobile robots with nonholonomic constraints," *IEEE Trans. Automat. Contr.*, vol. 37, pp. 1791–1797, Nov. 1992.

[6] O. J. Sørdalen, Y. Nakamura, and W. J. Chung, "Design of a Nonholonomic Manipulator," in *Proc. 1994 IEEE Int. Conf. Robotics and Automation*, San Diego, CA, May 1994, pp. 8–13.

[7] W. Chung and Y. Nakamura, "Design of the Chained Form Manipulator," in *Proc. 1997 IEEE Int. Conf. Robotics and Automation*, Albuquerque, NM, Apr. 1997, pp. 455–461.

[8] ——, "Experimental Research of the chained form manipulator," in *Proc. 1998 IEEE/RSJ Int. Conf. Intelligent Robots and Systems*, Victoria, BC, Canada, Oct. 1998, pp. 1027–1033.

[9] J. E. Colgate, M. Peshkin, and W. Wannasuphoprasit, "Nonholonomic haptic display," in *Proc. 1996 IEEE Int. Conf. Robotics and Automation*, Minneapolis, MN, Apr. 1996, pp. 539–544.

[10] J.-M. Coron, "Global asymptotic stabilization for controllable systems without drift," *Math. Control, Signals, Syst.*, vol. 5, pp. 295–315, 1991.

[11] L. Dubins, "On curves of minimal length with a constraint on average curvature and with prescribed initial and terminal positions and tangents," *Amer. J. Math.*, vol. 79, pp. 497–516, 1957.

[12] Y. Kawada *et al.*, *Handbook of the Strength of a Material* (in Japanese), 1 ed. Tokyo, Japan: Asakura, 1966.

[13] J. Godhavn and O. Egeland, "A lyapunov approach to exponential stabilization of nonholonomic systems in power form," *IEEE Trans. Automat. Contr.*, vol. 42, pp. 1028–1032, July 1997.

[14] L. Gurvits and Z. X. Li, "Smooth time-periodic feedback solutions for nonholonomic motion planning," in *Progress in Nonholonomic Motion Planning*, Z. X. Li and J. Canny, Eds. Norwell, MA: Kluwer, 1993, pp. 53–108.

[15] G. Lafferriere and H. J. Sussmann, "Motion planning for controllable systems without drift," in *Proc. 1991 IEEE Int. Conf. Robotics and Automation*, Sacramento, CA, Apr. 1991, pp. 1148–1153.

[16] J. P. Laumond, "Controllability of a multibody mobile robot," *IEEE Trans. Robot. Automat.*, vol. 9, pp. 755–763, Dec. 1993.

[17] J.-P. Laumond and T. Siméon, "Motion planning for a two degrees of freedom mobile robot with towing," in *Proc. Int. Conf. Control and Applications*, Jerusalem, Israel, Apr. 1989.

[18] Z. Li and J. Canny, "Motion of two rigid bodies with rolling constraint," *IEEE Trans. Robot. Automat.*, vol. 6, pp. 62–72, Feb. 1990.

[19] Z. Luo and M. Funaki, "Design and control of a cartesian nonholonomic robot" (in Japanese), *J. Robot. Soc. Jpn.*, vol. 15, no. 2, pp. 243–248, 1997.

[20] K. M. Lynch, "Locally controllable polygons by stable pushing," in *Proc. 1997 IEEE Int. Conf. Robotics and Automation*, Albuquerque, NM, Apr. 1997, pp. 1442–1447.

[21] A. Marigo, Y. Chitour, and A. Bicchi, "Manipulation of polyhedral parts by rolling," in *Proc. 1997 IEEE Int. Conf. Robotics and Automation*, Albuquerque, NM, Apr. 1997, pp. 2992–2997.

[22] R. T. M'Closkey and R. M. Murray, "Convergence rates for nonholonomic systems in power form," in *Proc. American Control Conf.*, San Fransisco, CA, June 1993, pp. 2967–2972.

[23] ——, "Exponential stabilization of driftless nonlinear control systems using homogeneous feedback," *IEEE Trans. Automat. Contr.*, vol. 42, pp. 614–628, May 1997.

[24] S. Monaco and D. Normand-Cyrot, "An introduction to motion planning under multirate control," in *Proc. IEEE 31th Conf. Decision and Control*, Tucson, AZ, Dec. 1992, pp. 1780–1785.

[25] R. M. Murray, "Applications and extensions of goursat normal form to control of nonlinear systems," in *Proc. 32th Conf. Decision and Control*, San Antonio, TX, Dec. 1993, pp. 3425–3430.

[26] R. M. Murray and S. S. Sastry, "Nonholonomic motion planning: Steering using sinusoids," *IEEE Trans. Automat. Contr.*, vol. 38, pp. 700–716, May 1993.

[27] Y. Nakamura and R. Mukherjee, "Nonholonomic path planning of space robots via bi-directional approach," *IEEE Trans. Robot. Automat.*, vol. 7, pp. 500–514, Apr. 1991.

[28] Y. Nakamura and S. Savant, "Nonlinear tracking control of autonomous underwater vehicles," in *Proc. 1992 IEEE Int. Conf. Robotics and Automation*, Nice, France, May 1992, pp. A4–A9.

[29] J. I. Neimark and N. A. Fufaev, "Dynamics of Nonholonomic Systems," in *Translations of Mathematical Monographs*: Amer. Mathematical Soc., 1972, vol. 33.

[30] T. Noguchi, "A new type of the harmonic analyzer" (in Japanese), *J. Jpn. Soc. Mech. Eng.*, vol. 27, no. 91, pp. 975–984, 1923.
[31] M. Peshkin, J. E. Colgate, and C. Moore, "Passive robots and haptic displays based on nonholonomic elements," in *Proc. 1996 IEEE Int. Conf. Robotics and Automation*, Minneapolis, MN, Apr. 1996, pp. 551–556.
[32] J.-P. Pomet, "Explicit design of time-varying stabilizing control laws for a class of controllable systems without drift," *Syst. Contr. Lett.*, vol. 18, no. 2, pp. 147–158, 1992.
[33] J. A. Reeds and L. A. Shepp, "Optimal paths for a car that goes both forward and backward," *Pacific J. Math.*, vol. 145, no. 2, pp. 367–393, 1990.
[34] M. Sampei, "A control strategy for a class of nonholonomic systems—time-state control form and its application," in *Proc. 33rd Conf. Decision and Control*, Lake Buena Vista, FL, Dec. 1994, pp. 1120–1121.
[35] M. Sampei, H. Kiyota, M. Koga, and M. Suzuki, "Necessary and sufficient conditions for transformation of nonholonomic system into time-state control form," in *Proc. 35th Conf. Decision and Control*, Kobe, Japan, Dec. 1996, pp. 4745–4746.
[36] C. Samson, "Control of chained systems application to path following and time-varying point-stabilization of mobile robots," *IEEE Trans. Automat. Contr.*, vol. 40, pp. 64–77, 1995.
[37] O. J. Sørdalen, "Conversion of the kinematics of a car with n trailers into a chained form," in *Proc. 1993 IEEE Int. Conf. Robotics and Automation*, Atlanta, GA, May 1993, pp. 382–387.
[38] ——, "Feedback Control of Nonholonomic Mobile Robots," Ph.D. dissertation, Norwegian Inst. Technol., ITK-rapport 1993:5-W, Feb. 1993.
[39] O. J. Sørdalen and O. Egeland, "Exponential stabilization of chained nonholonomic systems," in *Proc. 2nd Eur. Control Conf.*, Groningen, The Netherlands, June 1993.
[40] ——, "Exponential stabilization of chained nonholonomic systems," *IEEE Trans. Automat. Contr.*, vol. 40, pp. 35–49, Jan. 1995.
[41] O. J. Sørdalen, Y. Nakamura, and W. J. Chung, "Control of a nonholonomic manipulator," *Preprints of the 4 IFAC Symp. on Robot Control'94*, pp. 323–328, Sept. 1994.
[42] O. J. Sørdalen and K. Y. Wichlund, "Exponential stabilization of a car with n trailers," in *Proc. 32th Conf. Decision and Control*, San Antonio, TX, Dec. 1993, pp. 978–983.
[43] S. Timoshenko and J. N. Goodier, *Theory of elasticity*, 2 ed. New York: McGraw-Hill, 1951.
[44] T. Suzuki and Y. Nakamura, "Planning Spiral Motion of Nonholonomic Space Robots," in *Proc. 1996 IEEE Int. Conf. on Robotics and Automation*, Minneapolis, MN, Apr. 1996, pp. 718–725.
[45] A. R. Teel, R. M. Murray, and G. Walsh, "Nonholonomic control systems: From steering to stabilization with sinusoids," in *Proc. 31th Conf. on Decision and Control*, Tucson, AZ, Dec. 1992, pp. 1603–1609.
[46] D. Tilbury, J. P. Laumond, R. Murray, S. Sastry, and G. Walsh, "Steering car-like systems with trailers using sinusoids," in *Proc. 1992 IEEE Int. Conf. Robotics and Automation*, Nice, France, May 1992, pp. 1993–1998.
[47] D. Tilbury, R. Murray, and S. Sastry, "Trajectory generation for the n -trailer problem using goursat normal form," *IEEE Trans. Automat. Contr.*, vol. 40, pp. 802–819, May 1995.
[48] W. Flűgge, *Handbook of Engineering mechanics*, 1 ed. New York: McGraw-Hill, 1962.
[49] G. Walsh, D. Tilbury, S. Sastry, R. Murray, and J. P. Laumond, "Stabilization of trajectories for systems with nonholonomic constraints," in *Proc. 1992 IEEE Int. Conf. Robotics and Automation*, Nice, France, May 1992, pp. 1999–2004.
[50] ——, "Stabilization of trajectories for systems with nonholonomic constraints," *IEEE Trans. Automat. Contr.*, vol. 39, pp. 216–222, Jan. 1994.
[51] W. Wannasuphoprasit, R. B. Gillespie, J. E. Colgate, and M. A. Peshkin, "Cobot control," in *Proc. 1997 IEEE Int. Conf. Robotics and Automation*, Albuquerque, NM, Apr. 1997, pp. 3571–3576.

Yoshihiko Nakamura (M'87) was born in Osaka, Japan, in 1954. He received the B.S., M.S., and Ph.D. degrees from Kyoto University, Japan, in precision engineering in 1977, 1978, and 1985, respectively.

He was an Assistant Professor at the Automation Research Laboratory, Kyoto University, from 1982 to 1987. He joined the Department of Mechanical and Environmental Engineering, University of California, Santa Barbara (UCSB), in 1987, as an Assistant Professor, and became an Associate Professor in 1990. He was a Co-Director of the Center for Robotic Systems and Manufacturing at UCSB. Since 1991, he has been with the Department of Mechano-Informatics, University of Tokyo, Tokyo, Japan, and is currenly a Professor. He is currently conducting the research on brain-like information processing for humanoid robots under the CREST project of the Japan Science Corporation. He is the author of the textbook, *Advanced Robotics: Redundancy and Optimization* (Reading, MA: Addison-Wesley). His fields of research include redundant manipulators, actuation redundancy of closed kinematic chains, multirobot coordination, multifingered robot hands, space robot control, motion control of mechanical systems with nonholonomic constraints, and medical robotics.

Dr. Nakamura is a member of the ASME, the SICE, the Japan Robotic Society, the Japan Society of Mechanical Engineers, the Institute of Systems, Control, and Information Engineers, and the Japan Society of Computer Aided Surgery. He received Excellent Paper Awards from the Society of Instrument and Control Engineers (SICE) in 1985 and from the Robotics Society of Japan in 1996 and 2000.

Woojin Chung was born in Seoul, Korea, in 1970. He received the B.S. degree from the Department of Mechanical Design and Production Engineering, Seoul National University, Seoul, Korea, in 1993. He received the M.S. and Ph.D. degrees in 1995 and 1998, respectively, from the Department of Mechano-Informatics, the University of Tokyo, Tokyo, Japan.

Currently, he is a Senior Research Scientist with the Advanced Robotics Research Center, Korea Institute of Science and Technology, Korea. His research interests include the design and control of nonholonomic underactuated mechanical systems, trailer system design and control, mobile robot navigation, and a dexterous robot hand.

Dr. Chung received an Excellent Paper Award from the Robotics Society of Japan in 1996.

Ole Jacob Sørdalen (M'92) was born in Kragerø, Norway, in 1965. He received the Diploma Engineer(Siv.Ing) degree in 1988 and the Dr.Ing.degree in 1993 in electrical engineering and computer sciences at the Norwegian Institute of Technology, Trondheim, Norway.

From July 1993 through June 1994, he was a Visiting Researcher with the Department of Mechano-Informatics, University of Tokyo, Tokyo, Japan, with a fellowship from the Japan Society for the Promotion of Science. In addition, he has held visiting appointments at the Laboratoire d'Automatique de Grenoble, Grenoble, France, and the University of California, Berkeley. Currently, he is Program Manager for the ABB R&D program "Control and Optimization" with ABB Corporate Research. In addition, he is Adjunct Professor with the Department of Engineering Cybernetics, Norwegian University of Science and Technology, Trondheim, Norway.